BIOLOGY LETTERS

rsbl.royalsocietypublishing.org

Research

Cite this article: Liu Y, Roll J, Van Kooten S, Deng X. 2018 Schlieren photography on freely flying hawkmoth. *Biol. Lett.* **14**: 20180198.
http://dx.doi.org/10.1098/rsbl.2018.0198

Received: 21 March 2018
Accepted: 20 April 2018

Subject Areas:
bioengineering, biomechanics

Keywords:
insect flight, flow visualization, vortex structure, *Schlieren*

Author for correspondence:
Xinyan Deng
e-mail: xydengresearch@gmail.com

Electronic supplementary material is available online at https://dx.doi.org/10.6084/m9.figshare.c.4084115.

THE ROYAL SOCIETY PUBLISHING

Biomechanics

Schlieren photography on freely flying hawkmoth

Yun Liu[1], Jesse Roll[2], Stephen Van Kooten[2] and Xinyan Deng[2]

[1]Department of Mechanical and Civil Engineering, Purdue University Northwest, Westville, IN 46391, USA
[2]School of Mechanical Engineering, Purdue University, 585 Purdue Mall, West Lafayette, IN 47906, USA

XD, 0000-0001-8694-7833

The aerodynamic force on flying insects results from the vortical flow structures that vary both spatially and temporally throughout flight. Due to these complexities and the inherent difficulties in studying flying insects in a natural setting, a complete picture of the vortical flow has been difficult to obtain experimentally. In this paper, *Schlieren*, a widely used technique for high-speed flow visualization, was adapted to capture the vortex structures around freely flying hawkmoth (*Manduca*). Flow features such as leading-edge vortex, trailing-edge vortex, as well as the full vortex system in the wake were visualized directly. Quantification of the flow from the *Schlieren* images was then obtained by applying a physics-based optical flow method, extending the potential applications of the method to further studies of flying insects.

1. Introduction

The complex flow topology of flapping wings, revealed through smoke visualization conducted on insects and robotic flappers, established the prominence of a stably attached leading edge vortex (LEV) responsible for lift augmentation in insect flight [1,2]. Further characterized by scaled tank experiments with robotic flappers, quantitative force data were correlated to models of the quasi-steady aerodynamic mechanisms formulated from detailed oil tank experiments [3]. In the light of flow quantification techniques, e.g. particle image velocimetry (PIV), the study of flapping wing aerodynamics progressed to enable a quantitative depiction and measurements of flow structures generated by flying animals [4–6]. These flow investigations typically consisted of localized two-dimensional flow measurements, providing significant insight into the nature of animal flight, but they were limited in their depiction of three-dimensional vortex systems. Most recently, with the advancements in tomographic-PIV, the instantaneous vortical flow structure was successfully captured and reconstructed three-dimensionally on a tethered locust [7]. Nonetheless, only flow in the far-field, away from the tethered locust, was studied due to the inherent limitations of the method. Qualitative flow visualization methods, on the other hand, have been used to visualize three-dimensional flow in flying animals [8–10]. Smoke plume visualization on a hovering hummingbird was used to reconstruct the near-field three-dimensional flow structure in the downwash [8]. Yet, these visualization methods only depict patterns of streak-lines in the unsteady flow, leaving the vortex structures to be later interpreted from the complex smoke patterns [11]. Here we apply *Schlieren* photography, a widely used flow visualization method in high speed flow [12], on freely flying hawkmoth (*Manduca sexta*), using alcohol vapour as a passive scalar [11] to capture and visualize the three-dimensional vortex system. A physics-based optical flow method [13] is then used to quantify the near-field flow around the wing tip, demonstrating the potential of the method in further studies on flying insects.

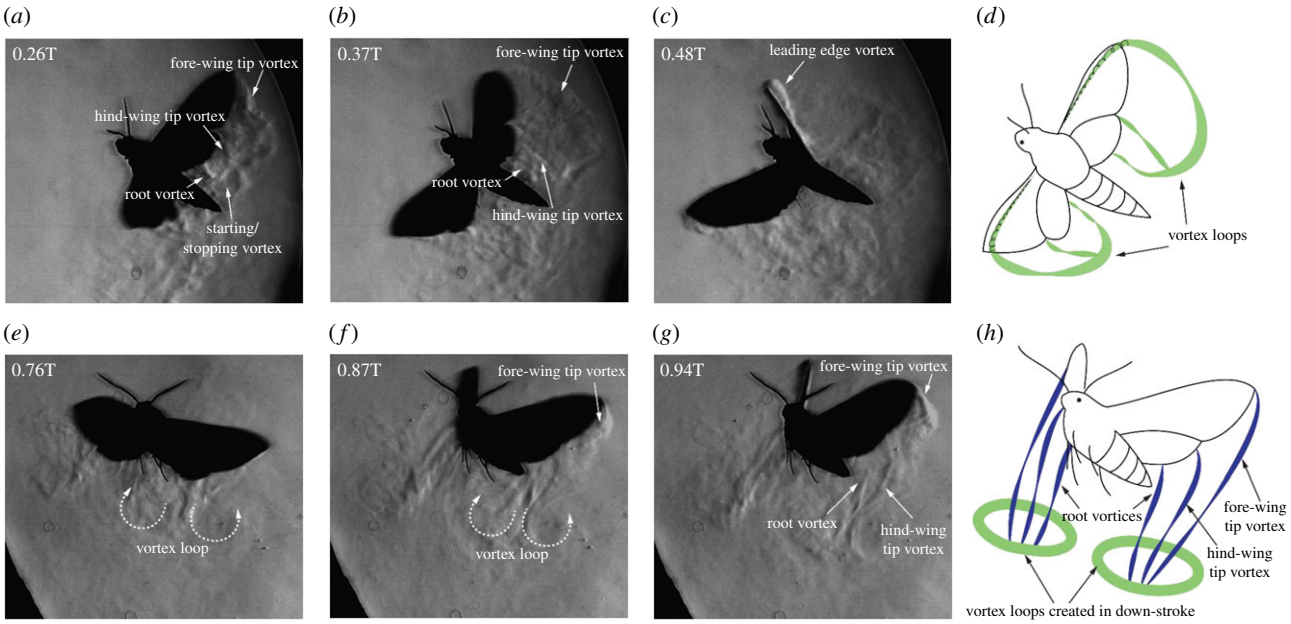

Figure 1. Vortex structures captured on a near-hovering male hawkmoth (1.26 g) with an average flying speed of 0.3 m s^{-1}. (*a*) A combined structure of starting/stopping vortex after wing pronation. (*b*) Tip vortices created from tips of fore and hind-wings. (*c*) An attached cone-shaped leading edge vortex before wing supination. (*d*) An illustrative depiction of the vortex structure created in the down-stroke. (*e*) The vortex loop created in the down-stroke sheds into the wake. (*f*–*g*) Long, stretched tip vortices generated from the tips of fore- and hind-wings and connected to the shed vortex loops. (*h*) An illustrative depiction of the vortex structure created in the up-stroke.

2. Material and methods

Male *Manduca sexta* adults were obtained from the Purdue University Entomology department. A high speed *Schlieren* photography system was implemented to visualize the unsteady three-dimensional vortical flow on freely flying *Manduca*. This system consists of two single mirror, double-pass, *Schlieren* set-ups with two high speed cameras (Mini UX100, Photron), filming from two orthogonal views. In each *Schlieren* system, a white LED light was projected through a 1 mm pin hole onto a 10-inch diameter optical spherical mirror (Edmond optics). A portion of the reflected light was then redirected towards the highspeed camera using a 50/50 (reflection/transmission ratio, Edmond optics) beam-splitter for capture. At the focal point of the reflected light, a razor blade was used as the knife-edge producing the *Schlieren* images (see electronic supplementary material, figure S1). To trace the vortical flow produced by the flapping *Manduca* wings, warm isopropyl alcohol (91% isopropyl alcohol heated to 38°C) was brushed onto the surface of both wings at the beginning of each test. The *Manduca* was then released to fly freely in the flow observation region. Upon wing acceleration and rotation, airflow over the wing surface increases vaporization of the alcohol, drawing it into the vortex sheet/vortices and forming the pattern of passive scalar. The *Schmidt* number of vaporized median is estimated to be on the order of one, thus formations depicted by the alcohol vapour will accurately capture the vortical flow structures in the absence of significant vortex stretching [11]. Through our high speed *Schlieren* photography system, the unsteady three-dimensional vortex structure was visualized and recorded by two high speed cameras at 1000 frames per second from two orthogonal views. In total, thirty tests were conducted and results from the most illustrative test are presented in this paper. The moth's average translating speed was measured by tracking an eye of the *Manduca* using a Matlab code developed by Hedrick [14].

3. Results

Using isopropyl alcohol applied to the surface of insect wings and high speed *Schlieren* photography, the overall vortex structure and its development on freely flying hawkmoth *Manduca sexta* can be directly visualized experimentally. Images of distinct vortex structures were obtained on a near hovering *Manduca* with an average flying speed of 0.3 m s^{-1} (measured by tracking the hawkmoth eye's motion over 300 image frames).

Figure 1*a*–*d* shows the images of vortex structure in the down-stroke. A combined structure of starting vortex and stopping vortex was observed on each wing in the beginning of down-stroke right after wing pronation (figure 1*a*). Then very quickly, on each wing, distinct tip vortices were generated from both the fore- and hind-wing (figure 1*b*). Meanwhile, a stable leading-edge vortex was created with one end connecting to the fore-wing tip vortex. Although a continuous leading-edge vortex extending across the thorax was previously reported by Bomphrey *et al.* [15] from experiments on tethered *Manduca* in a wind tunnel, we found no evidence of such a structure; instead, a cone-shaped leading edge vortex was observed (figure 1*c*) on each wing. This difference might be caused by the incoming flow velocity difference between the two experimental cases. As a result, an open vortex loop or horseshoe-shaped vortex [1] is created on each wing, connecting the leading-edge vortex, tip vortex, starting/stopping vortex and root vortex (figure 1*d*). (Video of the vortex structure in down-stroke can be found in the video file: 1.WMV; see Dryad repository: https://doi.org/10.5061/dryad.6rv7470.) This vortex loop structure on *Manduca* has been previously observed in experimental and numerical studies on *Manduca* models [1,16]. Having never been observed on freely flying *Manduca* directly, the observance of the vortex structure presented in this work thus serves as a direct confirmation of these studies. Furthermore, unique to previous experimental and numerical studies on *Manduca*, the existence of a secondary hind-wing tip vortex as revealed by this technique presents a more complete depiction of the vortex loop structures generated by the *Manduca* wings. At the end of the down-stroke, during the supination (figure 1*c*), the cone-shaped leading edge

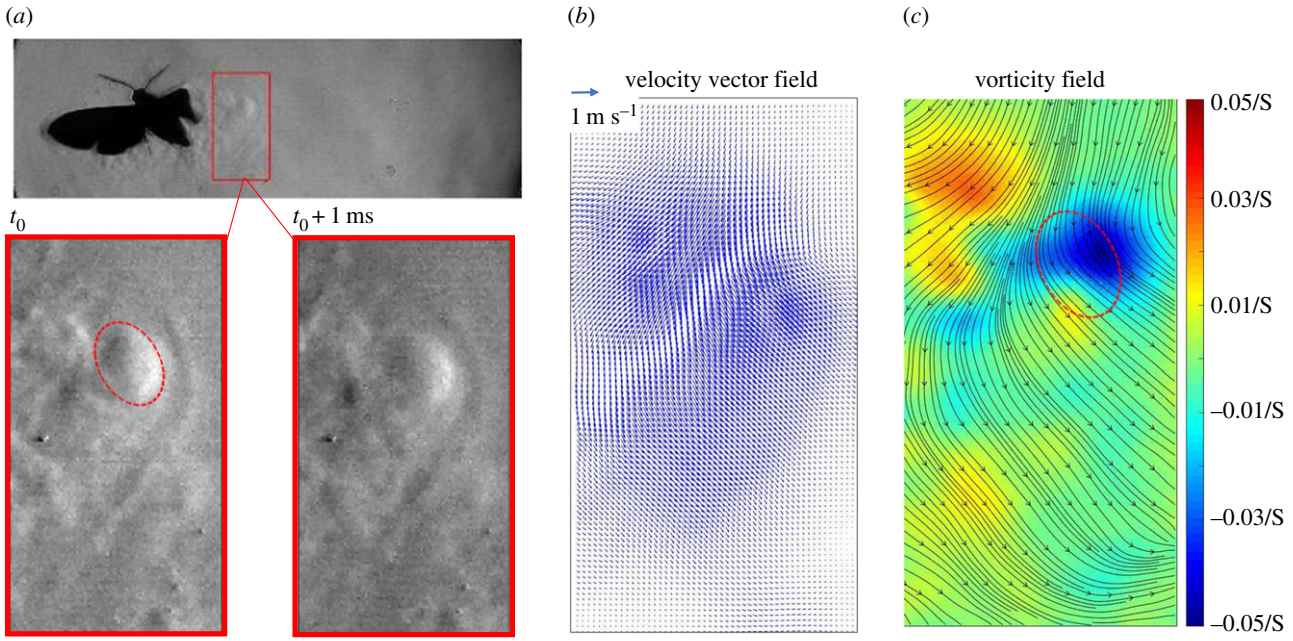

Figure 2. Velocity field quantification around wing tip. (*a*) Original *Schlieren* image with flow quantification region highlighted by red rectangle. The tip vortical flow image at a time instant is shown in the bottom left, while the tip vortical flow image in the next frame is shown in the bottom right. The tip vortex is highlighted by the red dashed loop. (*b*) Velocity vector field quantified using physics-based optical flow method. (*c*) Vorticity contour plot and streamline plot derived from the velocity quantification. Red dashed line from (*a*) matches well with the strong counter-clock vorticity.

vortex, under significant deformation due to the rapid wing twisting, was clearly captured. Subsequently, the leading-edge vortex is shed into the wake along with the other vortices created during the down-stroke, forming a closed vortex loop.

The vortex structure during the upstroke is shown in figure 1*e–h*. After wing supination, a closed vortex loop was shed into the wake from each wing while two significant tip vortices were created from the tips of fore- and hind-wings with ends connecting to the previously shed vortex loop (figure 1*g*). Concurrently, a root vortex was created, also connecting to the shed vortex loop. However, unlike the flow structure captured in the down-stroke, we found no evidence of a significant attached leading-edge vortex during the up-stroke. This is consistent with results from smoke visualization studies and computational fluid dynamics (CFD) simulations on a hovering *Manduca* model [1,16], and is indicative of a lack of vortex loop formation during the up-stroke. Therefore, after one complete wing beat cycle, the resulting vortex structure created under each wing consists of a vortex loop in the far wake, two tip vortices and a root vortex in the near field. (Video of the vortex structure in up-stroke can be found in the video file 2.WMV; see Dryad repository: https://doi.org/10.5061/dryad.6rv7470.)

As shown above, the vortical flow structures visualized by the isopropyl alcohol are distinctive features. The evolution and displacement of these features can be clearly seen through the provided videos. The physics-based optical flow method, appropriately suited as a velocity quantification tool for *Schlieren* images [13], is then applied on two consecutive images to quantify the flow velocity around the wing tip. Figure 2 presents an example of such flow velocity quantification using the method. First, the original *Schlieren* image with a clearly identified tip vortex highlighted by the red rectangular region is shown in figure 2*a*. Portions of two consecutive flow images (time interval of 1 ms) taken within the red rectangular region were then analysed using the physics-based optical flow method. A plot of the quantified velocity vectors field is provided in figure 2*b*, where a clear downward flow is measured with a maximum velocity of 0.6 m s^{-1}. In figure 2*c*, the vorticity contour and streamlines are plotted. The strong counter-clockwise vorticity region, shown in the blue, correlates with the tip vortex, highlighted by the red dashed region, demonstrating the method's ability to capture vortices.

Through *Schlieren* photography with isopropyl alcohol vapour as a medium, a linked vortex system is revealed on a freely flying *Manduca*. Similarly, linked vortical flow behaviours were observed through conventional flow visualizations and PIV measurements on birds and bats [8,17–19]. Using a stereo-PIV system, streamwise vorticity was quantified on freely flying blackcaps (*Sylvia atricapilla* L.) in a wind tunnel at different time instances and spatial locations, revealing a linked vortical flow structure in the wake region of the bird [17]. On a slowly flying bat, leading edge vortex, starting vortex, tip and root vortices were captured separately from the stream-wise and span-wise PIV measurements, suggesting a closed loop vortex system created during the down-stroke [18]. In our study, however, the entire vortex ring structure in the down-stroke was captured directly without the need for data reconstruction and interpretation. Furthermore, when paired with the physics-based optical flow method, quantification of vortical flow can be extended to the visualization images obtained through *Schlieren* photography. However, flow quantification of this type can only be used to quantify regions with strong vortical flow where the isopropyl alcohol vapour can be seen. Additionally, with limited numbers of cameras, the current physics-based optical flow method is restricted to flow quantification on the two-dimensional imaging plane and cannot quantify the flow in three-dimensional space. To extend this method to three-dimensional flow velocity quantification, *Schlieren* imaging from multiple views and advanced reconstruction algorithms are currently being explored.

Data accessibility. Video files 1.WMV, 2.WMV and figure S1 can be accessed through Dryad repository: https://doi.org/10.5061/dryad.6rv7470 [20].

Authors' contributions. Y.L. proposed this research idea, conducted the experiments with S.V.K. and wrote the paper together with J.R. and X.D. X.D. and J.R. were involved in the planning of the scientific and the technical aspects of the work. All authors gave final approval for publication and agree to be hold accountable for the work performed herein.

Competing interests. We claim no conflicting and competing interest in publishing this paper.

Funding. This work was funded by Air Force Office of Scientific Research (AFOSR) Grant number FA9550-11-1-0058.

Acknowledgements. We thank Prof. Sanjay P. Sane for his insight and expertise that assisted in this research. We would like to express our gratitude to Prof. Ian Kaplan and his student Michael Garvey for their help in hawkmoth raising and training. Additionally, we thank Prof. Tianshu Liu for his optical flow code and his help in analysing the images.

References

1. Van den Berg C, Ellington CP. 1997 The vortex wake of a 'hovering' model hawkmoth. *Phil. Trans. R. Soc. Lond. B* **352**, 317–328. (doi:10.1098/rstb.1997.0023)
2. Ellington CP, Van den Berg C, Willmott AP, Thomas ALR. 1996 Leading-edge vortices in insect flight. *Nature* **384**, 626–630. (doi:10.1038/384626a0)
3. Dickinson MH, Lehmann F, Sane SP. 1999 Wing rotation and aerodynamic basis of insect flight. *Science* **284**, 1954–1960. (doi:10.1126/science.284.5422.1954)
4. Pick S, Lehmann F. 2009 Stereoscopic PIV on multiple color-coded light sheets and its application to axial flow in flapping robotic insect wings. *Exp. Fluids* **47**, 1009–1023. (doi:10.1007/s00348-009-0687-5)
5. Johansson LC, Engel S, Kelbert A, Heerenbrink MK, Hedenstrom A. 2013 Multiple leading edge vortices of unexpected strength in freely flying hawkmoth. *Sci. Rep.* **3**, 3264. (doi:10.1038/srep03264)
6. Warrick DR, Tobalske BW, Powers DR. 2005 Aerodynamics of hovering hummingbird. *Nature* **435**, 1094–1097. (doi:10.1038/nature03647)
7. Henningsson P, Michaelis D, Nakata T, Schanz D, Geisler R, Schroder A, Bomphery RJ. 2015 The complex aerodynamic footprint of desert locusts revealed by large-volume tomographic particle image velocimetry. *J. R. Soc. Interface* **12**, 20150119. (doi:10.1098/rsif.2015.0119)
8. Pournazeri S, Segre PS, Princevac M, Altshuler DL. 2012 Hummingbirds generate bilateral vortex loops during hovering: evidence from flow visualization. *Exp. Fludis* **54**, 1439. (doi:10.1007/s00348-012-1439-5)
9. Bomphrey RJ, Taylor GK, Thomas ALR. 2009 Smoke visualization of free-flying bumblebees indicates independent leading-edge vortices on each wing pair. *Exp. Fluids* **46**, 811–821. (doi:10.1007/s00348-009-0631-8)
10. Thomas ALR, Taylor GK, Srygley RB, Nudds RL, Bomphrey RJ. 2004 Dragonfly flight: free flight and tethered flow visualizations reveal a diverse array of unsteady lift-generating mechanisms, controlled primarily via angle of attack. *J. Exp. Biol.* **207**, 4299–4323. (doi:10.1242/jeb.01262)
11. Smits AJ, Lim TT. 2012 *Flow visualization: techniques and examples*. London, UK: Imperial College Press.
12. Settles GS. 2011 *Schlieren and shadowgraph techniques*. Berlin, Germany: Springer.
13. Liu T, Shen L. 2013 Fluid flow and optical flow. *J. Fluid Mech.* **614**, 253–291. (doi:10.1017/S0022112008003273)
14. Hedrick TL. 2008 Software techniques for two- and three-dimensional kinematic measurements of biological and biomimetic systems. *Bioinspir. Biomim.* **3**, 034001. (doi:10.1088/1748-3182/3/3/034001)
15. Bomphrey RJ, Lawson NJ, Taylor GK, Thomas ALR. 2006 Application of particle image velocimetry to insect aerodynamics: measurement of the leading-edge vortex and near wake of a Hawkmoth. *Exp. Fluids* **40**, 546–554. (doi:10.1007/s00348-005-0094-5)
16. Zheng L, Hedrick TL, Mittal R. 2013 A multi-fidelity modelling approach for evaluation and optimization of wing stroke aerodynamics in flapping flight. *J. Fluid Mech.* **721**, 118–154. (doi:10.1017/jfm.2013.46)
17. Johansson C, Hedenström A. 2009 The vortex wake of blackcaps (*Sylvia atricapilla* L.) measured using high-speed digital particle image velocimetry (DPIV). *J. Exp. Biol.* **212**, 3365–3376. (doi:10.1242/jeb.034454)
18. Muijres FT, Johansson LC, Barfield R, Wolf M, Spedding GR, Hedenström A. 2008 Leading edge vortex improves lift in slow-flying bats. *Science* **319**, 1250–1253. (doi:10.1126/science.1153019)
19. Muijres FT, Johansson LC, Bowlin MS, Winter Y, Hedenström A. 2012 Comparing aerodynamic efficiency in birds and bats suggests better flight performance in birds. *PLoS ONE* **7**, e37335. (doi:10.1371/journal.pone.0037335)
20. Liu Y, Roll J, Van Kooten S, Deng X. 2018 Data from: Schlieren photography on freely flying hawkmoth. Dryad Digital Repository. (doi:10.5061/dryad.6rv7470)